Computer Methods and Programs in Biomedicine 218 (2022) 106724

Contents lists available at ScienceDirect

Computer Methods and Programs in Biomedicine

journal homepage: www.elsevier.com/locate/cmpb

# Effects of using different algorithms and fiducial points for the detection of interbeat intervals, and different sampling rates on the assessment of pulse rate variability from photoplethysmography

Elisa Mejía-Mejía*, James M. May, Panayiotis A. Kyriacou

*Research Centre for Biomedical Engineering, City, University of London, London, United Kingdom*

ARTICLE INFO

*Article history:*
Received 27 September 2021
Revised 28 February 2022
Accepted 28 February 2022

*Keywords:*
Photoplethysmography
Pulse rate variability
Fiducial points
Inter-beat intervals
Simulation

ABSTRACT

*Objective:* Pulse Rate Variability (PRV) has been widely used as a surrogate of Heart Rate Variability (HRV). However, there are several technical aspects that may affect the extraction of PRV information from pulse wave signals such as the photoplethysmogram (PPG). The aim of this study was to evaluate the effects of changing the algorithm and fiducial points used for determining inter-beat intervals (IBIs), as well as the PPG sampling rate, from simulated PPG signals with known PRV content.

*Methods:* PPG signals were simulated using a proposed model, in which PRV information can be modelled. Two independent experiments were performed. First, 5 IBIs detection algorithms and 8 fiducial points were used for assessing PRV information from the simulated PPG signals, and time-domain and Poincaré plot indices were extracted and compared to the expected values according to the simulated PRV. The best combination of algorithms and fiducial points were determined for each index, using factorial designs. Then, using one of the best combinations, PPG signals were simulated with varying sampling rates. PRV indices were extracted and compared to the expected values using Student t-tests or Mann-Whitney U-tests.

*Results:* From the first experiment, it was observed that AVNN and SD2 indices behaved similarly, and there was no significant influence of the fiducial points used. For other indices, there were several combinations that behaved similarly well, mostly based on the detection of the valleys of the PPG signal. There were differences according to the quality of the PPG signal. From the second experiment, it was observed that, for all indices but SDNN, the higher the sampling rate the better. AVNN and SD2 showed no statistical differences even at the lowest evaluated sampling rate (32 Hz), while RMSSD, pNN50, S, SD1 and SD1/SD2 showed good performance at sampling rates as low as 128 Hz.

*Conclusion:* The best combination of IBIs detection algorithms and fiducial points differs according to the application, but those based on the detection of the valleys of the PPG signal tend to show a better performance. The sampling rate of PPG signals for PRV analysis could be lowered to around 128 Hz, although it could be further lowered according to the application.

*Significance:* The standardisation of PRV analysis could increase the reliability of this signal and allow for the comparison of results obtained from different studies. The obtained results allow for a first approach to establish guidelines for two important aspects in PRV analysis from PPG signals, i.e. the way the IBIs are segmented from PPG signals, and the sampling rate that should be used for these analyses. Moreover, a model for simulating PPG signals with PRV information has been proposed, which allows for the establishing of these guidelines while controlling for other variables, such as the quality of the PPG signal.



## 1. Introduction

Pulse rate variability (PRV) refers to the changes in pulse rate (PR) overtime, when measured from pulse waves such as the photoplethysmogram (PPG), and has been widely used in recent

* Corresponding author.
*E-mail address:* elisa.mejia-mejia@city.ac.uk (E. Mejía-Mejía).

https://doi.org/10.1016/j.cmpb.2022.106724

decades as an alternative to heart rate variability (HRV) [1]. HRV assesses the changes of heart rate (HR) measured from the electrocardiogram (ECG) and has been used in different scenarios for evaluating the cardiac autonomic nervous system (ANS) and its regulation [2–4]. The assessment of PRV from PPG signals is increasingly gaining attention due to the widespread use of PPG sensors and their capability for obtaining cardiovascular information in a non-invasive, non-intrusive manner, in addition to the cost-effectiveness of the PPG devices [5].

Although HRV and PRV originate from similar processes, and pulse rate (PR) have been found to be a good surrogate of heart rate (HR) [6], the relationship between HRV and PRV is not straightforward, and there is still no consensus regarding the validity of using PRV as a surrogate of HRV [1]. Some researchers argue that the differences between HRV and PRV are mainly due to physiological aspects, such as changes of haemodynamics due to stress or disease [7–10], the different nature of PPG and ECG signals [1], and the effects on PRV of pulse transit time and other factors, e.g. external forces on the arterial vessels [11–13]. Moreover, PRV has been found to be present in the absence of HRV, as shown by Constant et al. [14] and Pellegrino et al. [15], and there are reports of differences in PRV due to measurement site [16,17]. All of these suggest there are different processes affecting PRV that are not related to HRV.

Besides physiological differences, other studies have concluded that the agreement between PRV and HRV may be affected by technical aspects in the extraction of PRV from pulse waves, such as the selection of fiducial points for the measurement of pulse-to-pulse intervals [18–20] and the sampling rate used for the acquisition of the pulse wave signals [21–23]. Moreover, there are no published guidelines for the extraction of PRV from pulse waves and the standardisation of the related analyses. Therefore, most methodologies for PRV studies are based on the guidelines for HRV assessment from ECG signals, published in 1996 [24].

The studies that have aimed to understand the effects of technical aspects on PRV results have been performed by comparing PRV to HRV, which might not be entirely correct due to the intrinsic differences between these two variables. The aim of this study was to establish guidelines for the selection of fiducial points and detection algorithms, as well as to study the effects of lowering sampling rate, on PRV indices extracted from simulated PPG signals, with known PRV values used as gold standards, instead of HRV extracted from ECG.

## 2. Materials and methods

### 2.1. Signal simulation

PPG signals were simulated applying a modified version of the model proposed by Tang et al. [25,26], which is based on modelling single PPG pulses as the combination of two Gaussian functions with specific parameters ($a_i$, $b_i$ and $\mu_i$) according to the quality of the PPG waveform. In the model proposed in this study, instead of altering the quality of the PPG waveform, it is possible to determine the ratio of the $a$ parameters, $r$, from the two Gaussian functions, which alters the amplitude of the function and, therefore the quality of the PPG cycle. The $b$ and $\mu$ parameters were selected according to what has been suggested in the original model [26]. The resulting model for the PPG cycle is shown in (1), where $\theta$ corresponds to the four quadrant inverse tangent of the cosine and sine functions of the duration of the cycle. In this study, both excellent and acceptable quality PPG signals were simulated, with ratios of $r = 2$ and $r = 4$, respectively.

$$z = a\left(e^{-\frac{(\theta-\mu_1)^2}{2b_1^2}}\right) + \frac{1}{r}a\left(e^{-\frac{(\theta-\mu_2)^2}{2b_2^2}}\right) \quad (1)$$

Fig. 1 illustrates the cardiac cycles generated using this model with the corresponding ratios for excellent and acceptable quality. The main difference between excellent and acceptable quality signals can be observed in the presence or absence of the dicrotic notch, and its amplitude when compared to the amplitude of the systolic peak.

An entire PPG signal with any duration can then be simulated by appending simulated pulses, each of them with a determined duration in order to generate the PRV information. The duration of each cardiac cycle was simulated using a sum of sinusoidal waves with randomly generated parameters that fall inside plausible physiological values. The ranges for these parameters are shown in Table 1. The resulting function for the randomly generated PRV information is shown in (2).

$$PRV = PR + SD\sum_{i=1}^{2}(\sin(2\pi LF(i)t) + \sin(2\pi HF(i)t)) \quad (2)$$

Each of the cardiac cycles simulated using (1), were concatenated to create the PPG signal and had a varying duration according to the sinusoidal wave generated using (2). As can be seen, the resulting PRV information contains two frequency components in the LF and HF bands. This was done to increase the variability of the frequency spectrum and to alter the area of each of the frequency bands. Further studies should aim to better simulate these components, but this was out of the scope of this study.

Using this model, PPG signals with varying qualities and with specific PRV content can be simulated. Fig. 2 depicts excellent and acceptable PPG signals simulated using the model with the specified $r$ values, and with known PRV information, which was randomly generated as sinusoidal signals with varying frequency and amplitude parameters. The randomly generated PRV information was considered as gold standard for this study. All simulated PPG signals had 1200 minutes cycles, which is longer than what is usually used for short-term PRV analysis and was considered sufficient to observe changes, especially in time-domain and Poincaré plot indices.

### 2.2. Experiment 1: Selection of the cardiac cycle detection algorithm and the fiducial point

#### 2.2.1. Inter-beat intervals detection algorithms and fiducial point extraction

A first experiment was conducted in order to assess changes in PRV extracted using different inter-beat intervals (IBIs) detection algorithms and fiducial points. In this experiment, 20-min PPG signals were simulated using a 2048 Hz sampling rate, in order to diminish the effects of a low sampling rate in the detection of the fiducial points. All data simulation and signal processing was performed in MATLAB (version 2020b).

Five algorithms available in the literature have been implemented for the extraction of inter-beat intervals from the simulated PPG signals, both with excellent and acceptable quality. The first of these algorithms, HeartPy, was proposed by van Gent et al. [27]. In this algorithm systolic peaks are detected using an adaptive threshold based on a moving average and the determination of regions of interest (ROIs). The threshold is adapted according to the instantaneous heart rate and the standard deviation of peak-to-peak intervals. At the end, detected peaks are corrected based on outlier detection and rejection using the ±30% of the mean duration of peak-to-peak intervals. The algorithm is robust against signal clipping and has low-computational load.

The second implemented algorithm was called D2max [28]. The first steps of this algorithm involve filtering, clipping and squaring the signal, before generating blocks of interest based on two moving averages, which are designed based on the expected duration

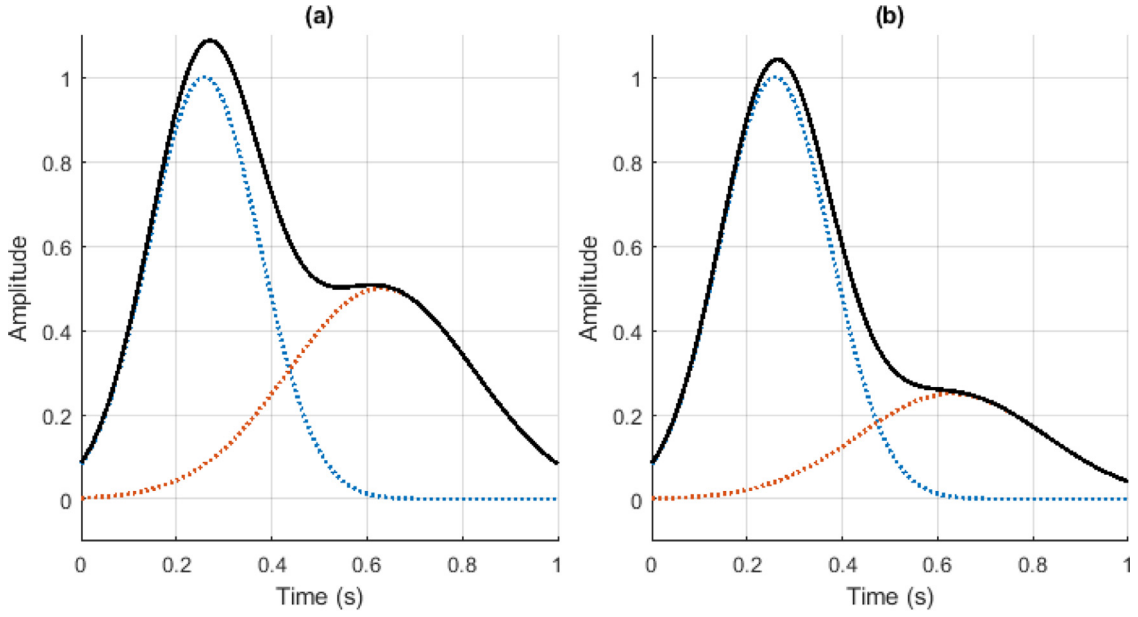


**Fig. 1.** Photoplethysmographic cardiac cycles generated using the proposed mode, using ratios of value (a) $r = 2$ (excellent quality), and (b) $r = 4$ (acceptable quality). The blue and orange dotted lines illustrate the two Gaussian functions generated, while the black continuous line shows the result of summing these two Gaussian functions, i.e., $z$.

**Table 1**
Ranges for the Pulse Rate Variability (PRV) parameters and the generation of PRV gold standard values.

| Parameter | Range | Units |
|---|---|---|
| Low frequency peak location (LF) | 0.04 - 0.15 | Hz |
| High frequency peak location (HF) | 0.15 - 0.40 | Hz |
| Average pulse rate (PR) | 40 - 200 | Beats per minute (bpm) |
| Standard deviation of pulse rate (SD) | 0.05 - 0.08 | s |

of cardiac cycles and the $a$ point in the second derivative of the PPG signal. The location of the systolic peak from the PPG signal is determined as the location of the maximum point in each block of interest. This algorithm has been shown to be robust against movement artifacts.

The algorithm proposed by Argüello Prada and Serna Maldonado has also been implemented in this study [29]. This algorithm, referred to as Upslopes, detects systolic upslopes instead of systolic peaks, since this is a constant feature of the PPG morphology regardless of the subject from which the signal is acquired or the body-site. The approach consists in identifying when there is an upslope in the signal, which is easily determined by checking if the amplitude of $i$-th sample of the signal is higher than the amplitude of the previous sample, $i - 1$. A counter is updated until the condition is not met, and the value of the counter determines if the portion of the signal corresponds to a new pulse or not, depending on a comparison threshold. If the counter is smaller than the threshold, the algorithm determines that the current upslope does not occur due to a new cardiac cycle and starts counting again from zero. This is a simple algorithm which could be applied in real-time embedded applications.

Another of the applied algorithms is based on the work proposed by Conn and Borkholder [30], which aims to identify the onset of the cardiac cycles using Wavelet transform. This method applies a fifth-scale quadratic spline Wavelet to the PPG, in which distinct peaks appear at the start of each beat. Using these peaks, a threshold is generated for identifying the valid range for the PPG onset, instead of the systolic peaks. Then, the third derivative of the PPG is obtained, and the first zero-crossing of this signal within the valid range is assigned as the onset of each pulse. Since it applies a Wavelet transform, this algorithm is robust to noise and shows high performance for the identification of PPG onsets.

Finally, the algorithm proposed by Li and Dong [31] for the detection of cardiac cycles from arterial blood pressure waveforms has been applied. The first stage of this algorithm applies a low pass filter and obtains the derivative of the signal. Thresholds are also estimated from the filtered signal. Using the first derivative of the signal, zero-crossings are detected, and beats are evaluated according to the estimated thresholds and the detected zero-crossings. Then, peaks and onsets are detected from each beat, and dicrotic notches are also detected using inflection detection. In this study, the resulting onsets from this algorithm were used to segment the interbeat intervals.

IBIs longer than 1.25 times the median duration of all the IBIs were corrected by looking for additional cardiac cycles in each of these longer windows. IBIs shorter than 0.75 times the median duration of IBIs were also detected and discarded. Then, eight fiducial points were obtained from each segmented cycle. The extracted fiducial points were the systolic peak (PKS); the onset, considered as the minimum point before the systolic peak (ONS); the onset determined as the intersection point between the tangent line crossing the onset and the tangent line crossing the maximum slope point (TI); the location of the maximum point in the first derivative of the PPG cycle (M1D); the $a$ and $b$ points from the second derivative of the PPG cycle (A and B, respectively); and the $p_1$ and $p_2$ points obtained from the third derivative of the PPG cycle (P1 and P2, respectively). These fiducial points have been previously described in the literature [32]. Fig. 3 illustrates the identification of these fiducial points in a segmented PPG cycle and its second and third derivatives.

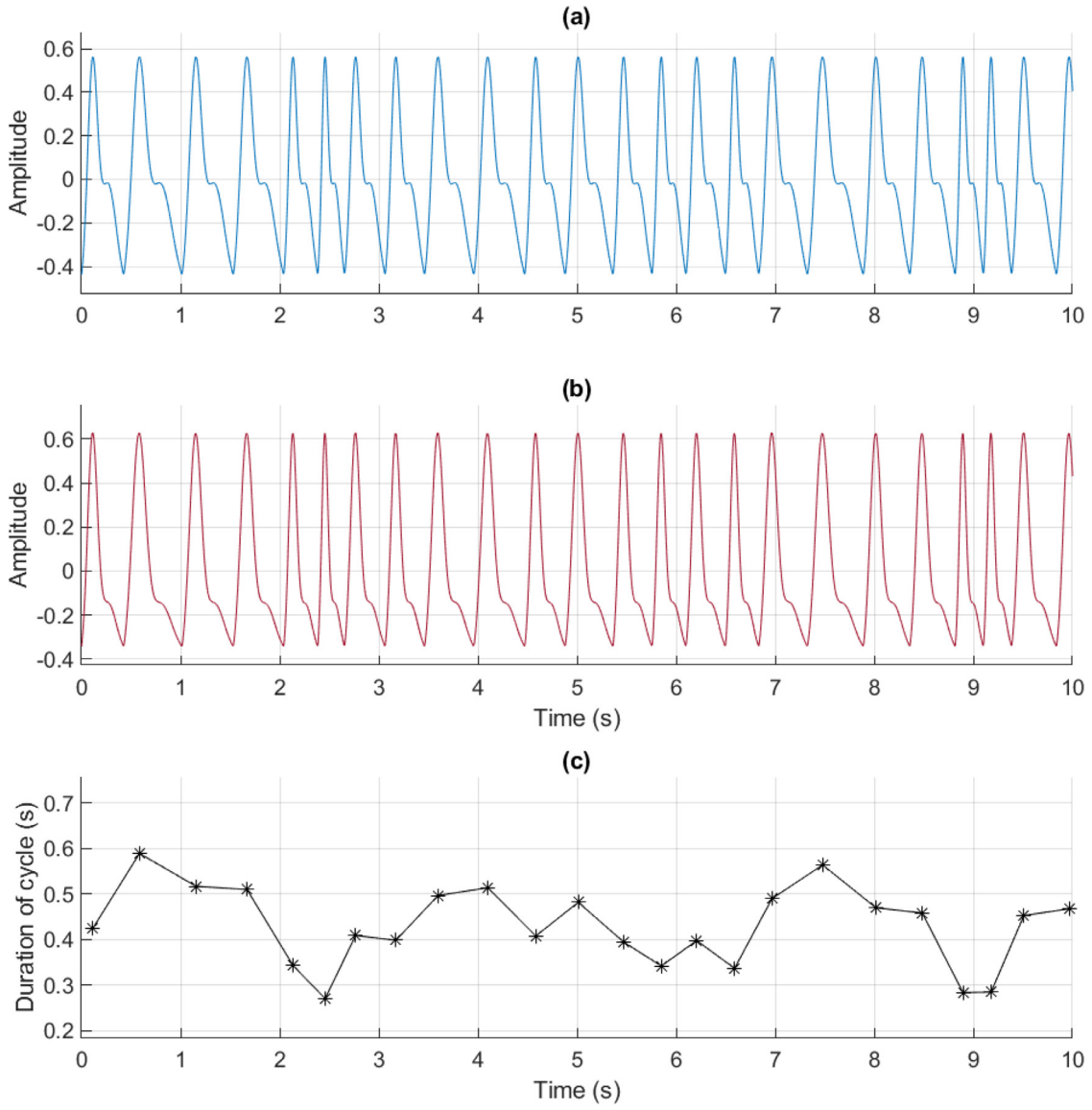


**Fig. 2.** Example of photoplethysmographic (PPG) signals simulated using the proposed model and randomly generated pulse rate variability (PRV) information. (a) PPG signal with excellent quality ($r = 2$). (b) PPG signal with acceptable quality ($r = 4$). (c) PRV information used for the generation of these signals.

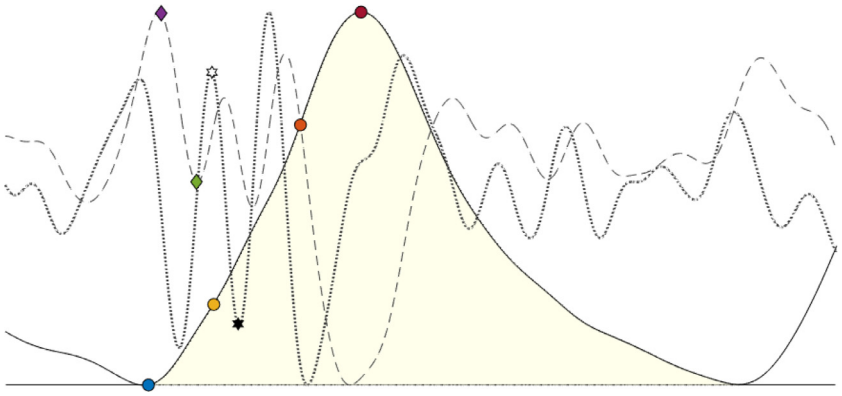

**Fig. 3.** Fiducial points extracted from each inter-beat interval detected from the photoplethysmographic signals (continuous line), its second derivative (dashed line) and third derivative (dotted line). Red circle: Systolic peak (PKS); blue circle: Onset (ONS); yellow circle: Tangent intersection point (TI); orange circle: Maximum slope point (M1D); purple diamond: *a* point from the second derivative (A); green diamond: *b* point from the second derivative (B); white star: $p_1$ point from the third derivative (P1); black star: $p_2$ point from the third derivative (P2).

*2.2.2. Extraction of pulse rate variability*

PRV trends were obtained as the duration of IBIs extracted from each of the fiducial points, which were in turn obtained from the cycles segmented using each of the IBI detection algorithms.

Both time-domain and Poincaré plot indices were obtained from each of the trends. Extracted time-domain indices were the average value of the normal-to-normal IBIs (AVNN), the standard deviation of the normal-to-normal IBIs (SDNN), the root mean square value of the successive difference of normal-to-normal IBIs (RMSSD), and the proportion of the successive differences of normal-to-normal IBIs that were longer than 50 ms (pNN50). The 1-lag Poincaré plot was obtained and the ellipse-fitting technique [33] was applied for the extraction of the area of the ellipse (S), the short- and long-term variability of the plot (SD1 and SD2, respectively), and the ratio between SD1 and SD2 (SD1/SD2).

*2.2.3. Sample size determination*

A pilot test was performed to determine the sample size needed to observe enough differences in the results, this was done as recommended in the literature [34]. A total of 384 PRV trends were generated randomly. Time-domain and Poincaré plot indices were extracted from the generated PRV information, considered as gold standard. Then, the sample size needed for the identification of differences as low as 2% of the mean value obtained for each of the indices was calculated applying (3) for differences of means, and used for AVNN, SDNN, RMSSD, S, SD1 and SD2, or (4) for differences of proportions and used for pNN50 and SD1/SD2 [35]. In this study, a sample size was obtained for each index with type I and II errors of $\alpha = 0.05$ and $\beta = 0.2$, respectively, and with $S$ estimated as the standard deviation of each index extracted from the PRV gold standard; $\mu_1$ as the mean value of each index extracted from the PRV gold standard; $\mu_2$ as 1.02 times $\mu_1$; $p_1$ as the mean value of the proportions obtained from the PRV gold standard; and $p_2$ as 1.02 times $p_1$.

$$n = \frac{2(Z_{\frac{\alpha}{2}} - Z_{\beta})S}{(\mu_1 - \mu_2)^2} \tag{3}$$

$$n = \frac{(Z_{\frac{\alpha}{2}}\sqrt{2p_2(1-p_2)} - Z_{\beta}\sqrt{p_1(1-p_1)+p_2(1-p_2)})^2}{(p_1 - p_2)^2} \tag{4}$$

A final resulting sample size of 125 signals was determined by selecting a value near the minimum of the resulting sample sizes obtained for the different indices, since a larger sample size can also lead to unreliable results in the statistical analyses [36,37].

*2.2.4. Identification of the best combination of factors*

PRV trends ($n = 125$) were randomly generated, and excellent and acceptable PPG signals were simulated considering these trends. These PRV trends are considered as the gold standard for the subsequent statistical analysis. IBIs were extracted from the simulated PPG signals using the five algorithms for the detection of IBIs, and PRV was assessed from each of the eight fiducial points. Both excellent and acceptable PPG signals were simulated. Since the aim of this experiment was to determine which algorithms and fiducial points allowed a more reliable estimation of PRV indices, compared to the indices extracted from the randomly generated PRV information, the differences between the indices extracted from the obtained PRV trends and the gold standard PRV were calculated, and Minitab (version 19.1) was then used to perform a factorial analysis to determine which differences were minimal. Since the data did not follow a normal distribution, a Box-Cox transformation [38] was applied before the analysis of variance (ANOVA) for each extracted index. In the cases in which the ANOVA showed a difference among factors, post-hoc analyses were performed using Bonferroni pairwise comparisons.

Lastly, to determine which combination of algorithms and fiducial points gave the lower differences between measured and gold standard PRV, the combinations of factors that delivered minimal differences were obtained for each index after determining which indices showed a significant interaction between algorithms and fiducial points.

*2.3. Experiment 2: Effects of lowering sampling rate for the extraction of pulse rate variability*

*2.3.1. Extraction of pulse rate variability*

A second experiment was conducted to evaluate the effects of lowering sampling rate changes in PRV extracted using the best combination of IBIs detection algorithms and fiducial points. PPG signals with duration of 20 minutes were simulated using sampling rates of 32 Hz, 64 Hz, 128 Hz, 256 Hz, 512 Hz, 1024 Hz and 2048 Hz. Then, the combination of IBIs detection algorithm and fiducial point that performed the best in the previous experiment for excellent and acceptable PPG signals, was used for extracting PRV trends and, similarly as in the first experiment, time domain and Poincaré plot indices were calculated from these trends, and from the gold standard PRV.

*2.3.2. Sample size determination*

As performed in the previous experiment, the sample size needed for the identification of differences as low as 2% of the results obtained from the gold standard PRV was determined using (3) and (4). This was done after simulating 384 PRV trends for each sampling rate. Then, the time domain and Poincaré plot indices were extracted from this PRV data, and the sample size for each of the indices and each of the sampling rates was determined. Again, the resulting sample size for this experiment was 125 signals.

*2.3.3. Evaluation of the effects of sampling rate on PRV assessment*

PRV trends ($n = 125$), which are considered as gold standard for this experiment, were randomly generated for each of the sampling rates considered in this study, and excellent and acceptable PPG signals were simulated using this information. Therefore, PPG signals were generated independently for each sampling rate, instead of resampling a single set of PPG signals simulated with a large sampling rate. From these simulated signals, PRV trends were extracted and time domain and Poincaré plot indices were measured. RStudio (version 1.1463) was used to compute the following statystical analyses; Student t-tests and Mann-Whitney tests were used for comparing the indices measured from the extracted and gold standard PRVs, for normally and non-normally distributed data, respectively, and normality was assessed using Lilliefors tests.

## 3. Results

*3.1. Experiment 1: Selection of the best combination of cardiac cycles detection algorithm and fiducial point*

After simulating the data, IBIs were extracted from each of these signals using the algorithms described above, and PRV trends were measured using each of the fiducial points shown in Fig. 3. From these trends and the gold standard PRV data, all the proposed indices were extracted and the difference between measurements was assessed. A summary of these differences is presented in Figs. 4 and 5, for excellent and acceptable PPG signals, respectively. Some of the extracted indices behave differently due to the algorithms used. For instance, there are differences in pNN50 and S among algorithms and signal quality. This needs to be considered when deciding what kind of algorithm to use for a specific analysis involving these two indices. On the other hand, differences among

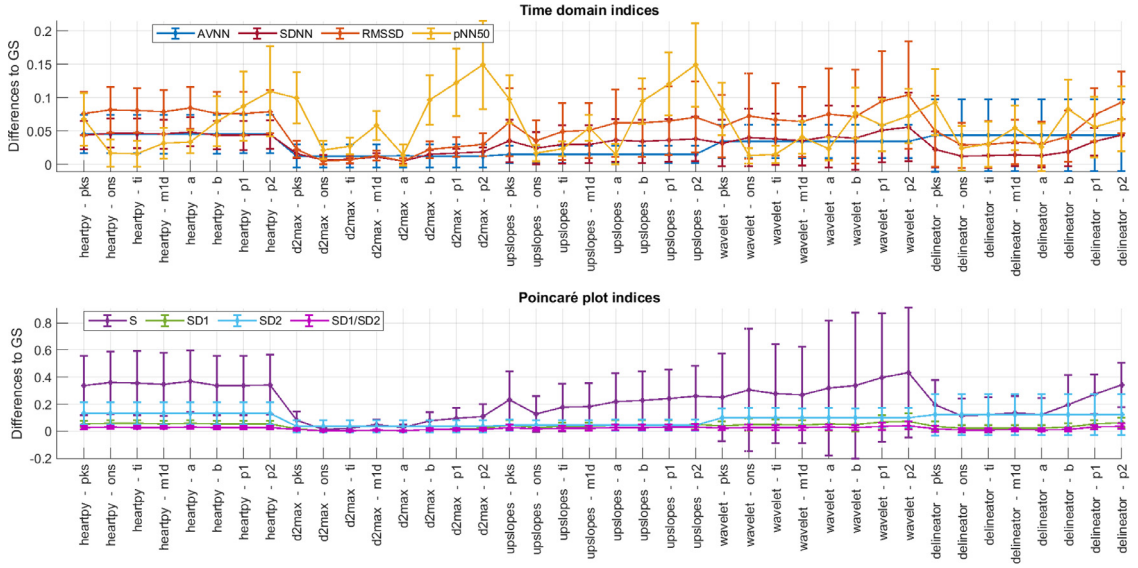


**Fig. 4.** Summary of the absolute differences between indices measured from gold standard and extracted pulse rate variability from excellent quality PPG signals.

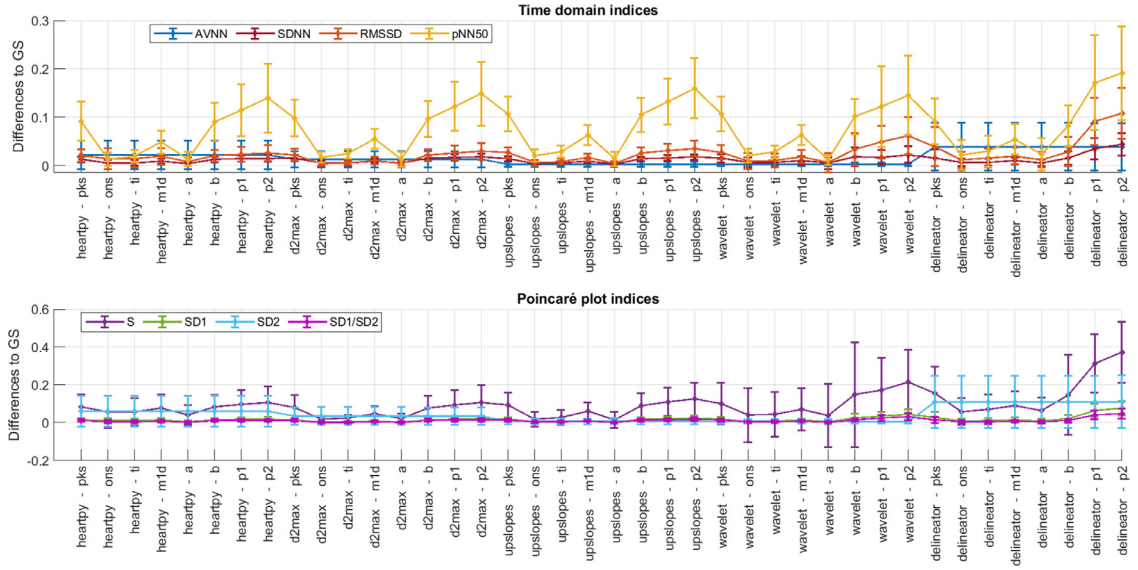


**Fig. 5.** Summary of the absolute differences between indices measured from gold standard and extracted pulse rate variability from acceptable quality PPG signals.

fiducial points within the same algorithm are not very significant for AVNN and SD2.

For each index, a factorial analysis was performed, to identify if there were differences among algorithms and fiducial points, and to assess whether the interaction between algorithm and fiducial point showed any statistical significance. Fig. 6 summarises the results obtained from these factorial analyses. It can be observed that AVNN and SD2 are the only indices in which the fiducial points or the interaction between algorithms and fiducial points are not statistically significant, while all indices have similar behaviour regardless of the quality of the signal, which could be due to the fact that all the fiducial points extracted in this study belong to the systolic phase of the cardiac cycle, and this is not highly affected by the difference in quality in the proposed model. Only fiducial points from the systolic phase were considered in this study due to the smooth changes and varying morphologies of the diastolic phase of the cardiac cycle obtained from PPG signals, and because the absence of a very distinct point in this phase could introduce additional errors in the analysis. Moreover, most of the PRV-related studies reported in the literature make use of the fiducial points included in the present study.

Since the aim of this experiment was to determine the best combination of fiducial points and algorithms used for PRV assessment, the differences between indices measured from gold standard and extracted PRV that did show significant interactions were determined and organised in ascending order (Figs. 7, 8, 9, 10, 11 and 12). In all cases, the minimum difference between indices obtained from gold standard and extracted PRV were obtained using D2Max, Upslopes or Wavelet algorithms, and using A and ONS fiducial points. It is also noticeable that there are differences in the best combination between excellent and acceptable PPG signals, with differences being lower in the acceptable quality signals only for SDNN analysis. Therefore, it is important to determine the algorithm and fiducial points to use in a given analysis considering also the quality of the signals used.

Then, post-hoc comparisons were performed among the 5 combinations that showed the lowest differences, to determine whether there was a significant difference among them (p-value

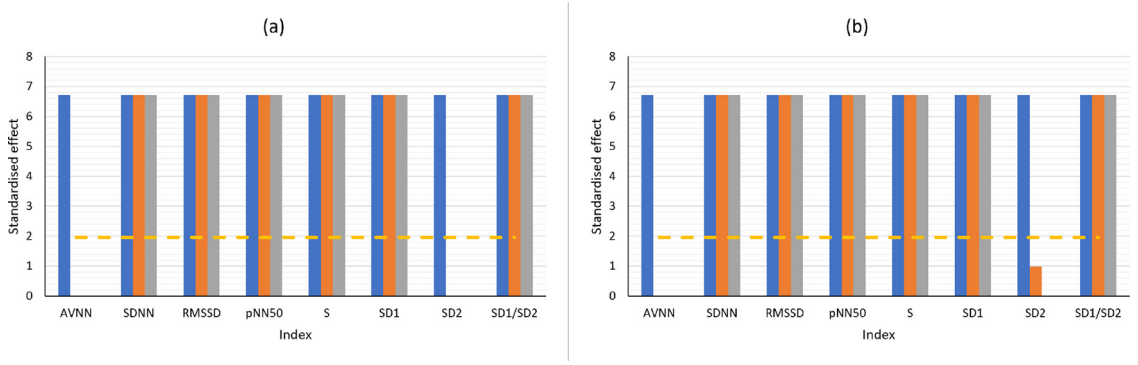


**Fig. 6.** Results obtained from the factorial analyses both with (a) excellent quality PPG signals and (b) acceptable quality PPG signals. Blue bars: Standardised effects of the algorithm. Orange bars: Standardised effects of the fiducial points. Grey bars: Standardised effects of the interaction between the two factors. Yellow line: Reference value; higher standardised effects imply significance of the factor or the interaction.

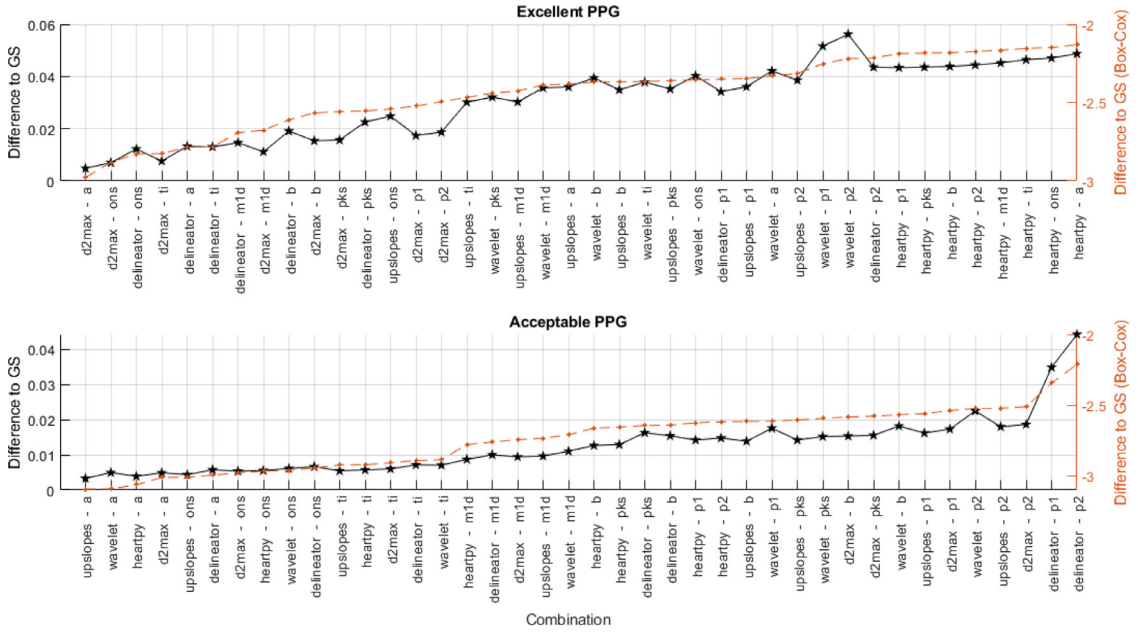


**Fig. 7.** Mean value of the absolute differences between SDNN measured from gold standard and extracted pulse rate variability (PRV), measured from excellent (top) and acceptable (bottom) quality photoplethysmographic signals. Left axis (black, continuous line): Difference to gold standard before Box-Cox transformations. Right axis (orange, dashed line): Difference to gold standard after Box-Cox transformation.

lower than 5%). These results are shown in Tables 2 and 3. For all indices, except for pNN50 obtained from acceptable PPG signals, the first three combinations with lowest differences do not show any statistical difference. For both excellent and acceptable PPG, D2max was the more frequent algorithm (15 out of 18 combinations), while Delineator for SDNN, and Wavelet and HeartPy for pNN50 also showed good performance. The only case in which D2max was not considered the best algorithm was for pNN50, in which Wavelet and HeartPy showed the best performance and did not have any statistically significant differences. When the fiducial points are considered, it can be seen that the A, ONS and TI points showed the best behaviour in all cases. There were statistically significant differences among these fiducial points only for pNN50 measured from acceptable PPG signals. However, the most frequency combination of algorithm and fiducial point that gave the lowest difference between gold standard and extracted PRV was D2max - A (8 out of 12 cases).

In summary, the algorithm with the best behaviour when compared to gold standard PRV was D2Max, while better results were obtained using the A point from the second derivative as fiducial point for extraction of interbeat intervals. In most applications, however, the TI and ONS points should give similarly good results.

### 3.2. Experiment 2: Effects of lowering sampling rate for the extraction of pulse rate variability

Fig. 13 summarises the time-domain and Poincaré plot indices extracted from the simulated data using different sampling rates. The red stars on top of the bars indicate statistically significant differences with the gold standard. In most cases, indices extracted from both acceptable and excellent quality simulated PPG signals showed lower values than those obtained from gold standard PRV. The standard deviation is similar among the groups and comparable in most cases as well. Importantly, the difference between gold standard and extracted PRV indices seem to remain stable for most of the sampling rates analysed, although differences become more noticeable for sampling rates below 128 Hz.

Most indices showed statistically significant differences to the gold standard when the sampling rate was 64 Hz, while above 256 Hz only SDNN showed statistically significant differences. The analyses performed in this experiment were based on the extraction

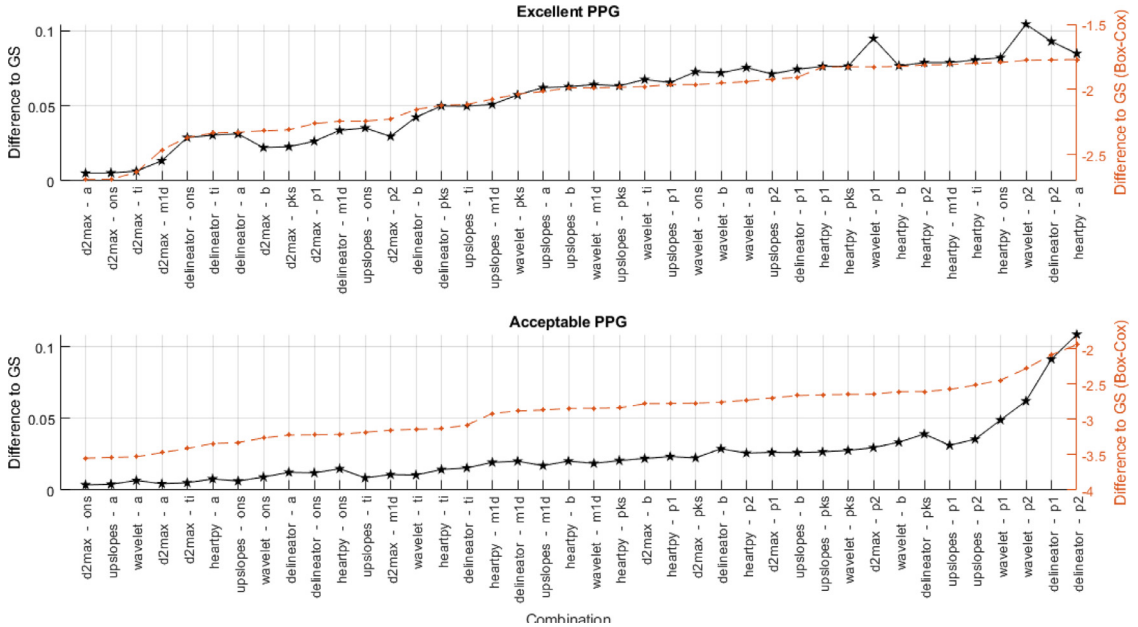


**Fig. 8.** Mean value of the absolute differences between RMSSD measured from gold standard and extracted pulse rate variability (PRV), measured from excellent (top) and acceptable (bottom) quality photoplethysmographic signals. Left axis (black, continuous line): Difference to gold standard before Box-Cox transformations. Right axis (orange, dashed line): Difference to gold standard after Box-Cox transformation.

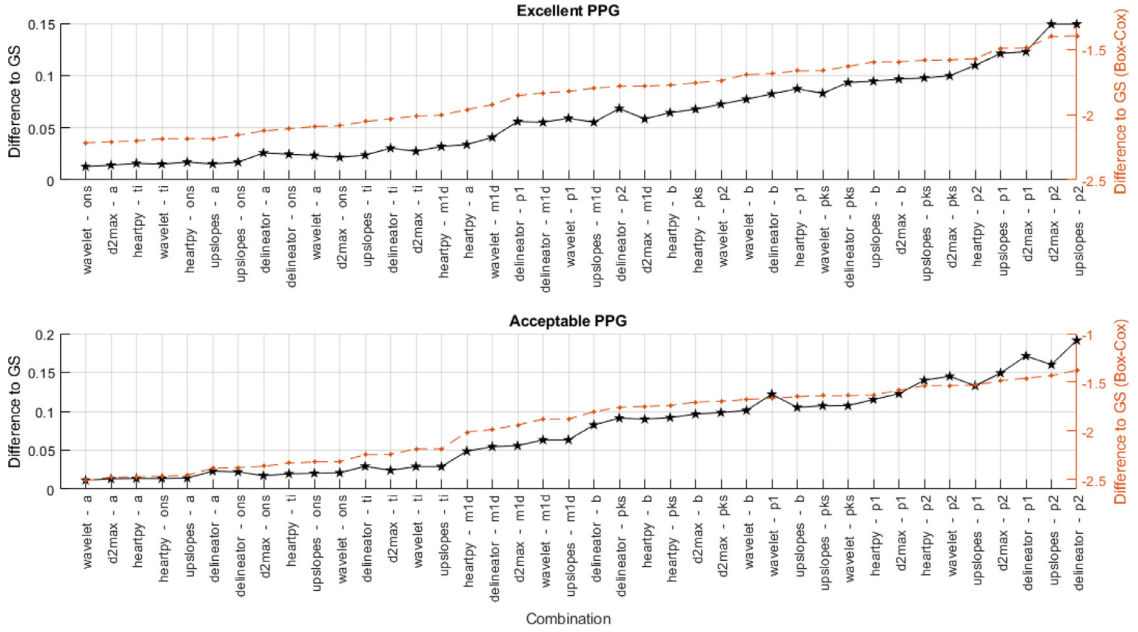


**Fig. 9.** Mean value of the absolute differences between pNN50 measured from gold standard and extracted pulse rate variability (PRV), measured from excellent (top) and acceptable (bottom) quality photoplethysmographic signals. Left axis (black, continuous line): Difference to gold standard before Box-Cox transformations. Right axis (orange, dashed line): Difference to gold standard after Box-Cox transformation.

of PRV information using inter-beat intervals detected with the D2Max algorithm, and the *a* point from the second derivative of PPG as fiducial point.

## 4. Discussion

PPG-based PRV has been proposed as an alternative to evaluate cardiovascular autonomic activity, instead of HRV acquired from ECG signals. However, the relationship between these two variables is not entirely understood, and there is evidence of both physiological and technical aspects that may affect PRV differently to HRV [1,6]. Moreover, although guidelines have been proposed for the extraction and analysis of HRV information from ECG signals [24], there is not a standard procedure for the analysis of PRV information from pulse wave signals, specifically from PPG. In this study, the aim was to evaluate how certain technical aspects, i.e. the extraction of inter-beat intervals from PPG signals and the sampling rate used for the acquisition of these signals, affect the assessment of time-domain and Poincaré plot indices from PRV. For this, a model for simulating PPG signals with varying PRV information was proposed, and two independent experiments were performed for evaluating the effects of these technical aspects on PRV assessment.

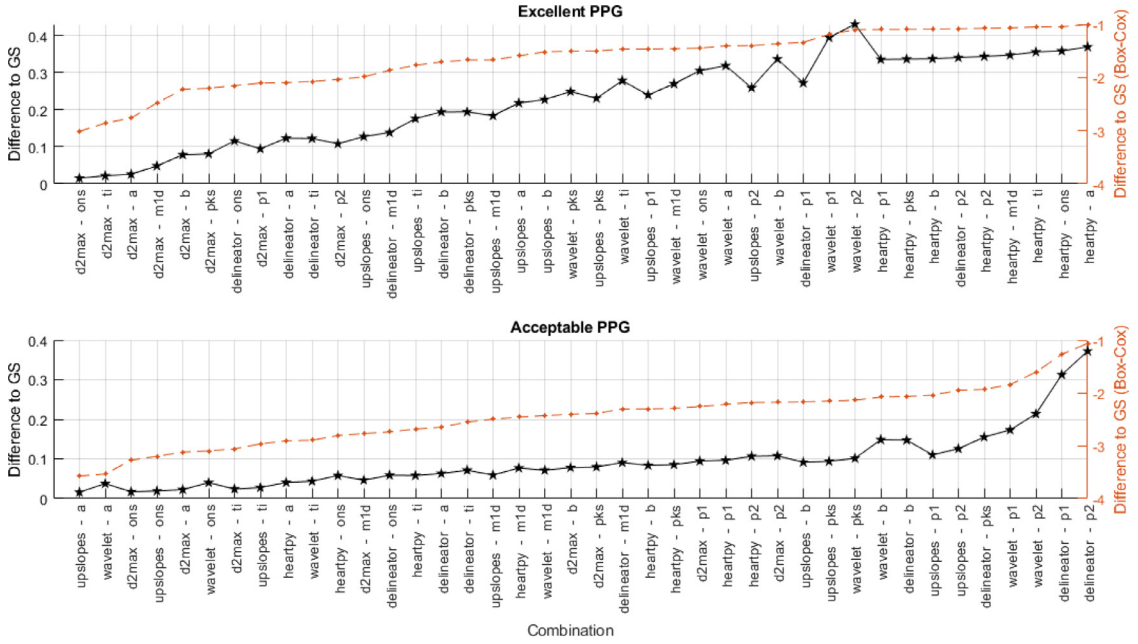


**Fig. 10.** Mean value of the absolute differences between S measured from gold standard and extracted pulse rate variability (PRV), measured from excellent (top) and acceptable (bottom) quality photoplethysmographic signals. Left axis (black, continuous line): Difference to gold standard before Box-Cox transformations. Right axis (orange, dashed line): Difference to gold standard after Box-Cox transformation.

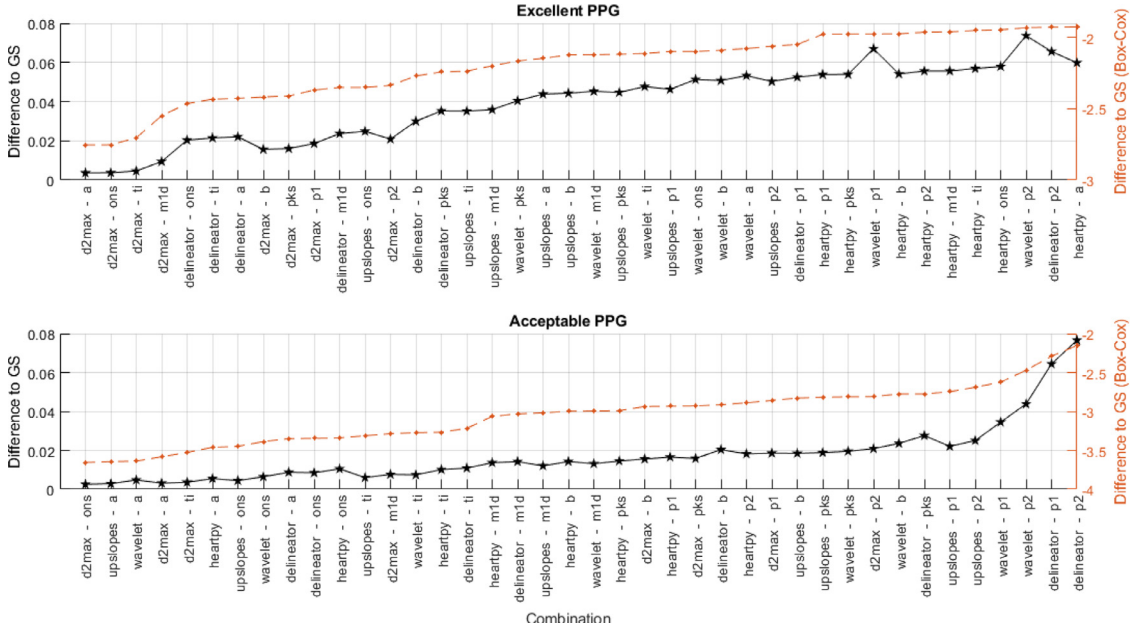


**Fig. 11.** Mean value of the absolute differences between SD1 measured from gold standard and extracted pulse rate variability (PRV), measured from excellent (top) and acceptable (bottom) quality photoplethysmographic signals. Left axis (black, continuous line): Difference to gold standard before Box-Cox transformations. Right axis (orange, dashed line): Difference to gold standard after Box-Cox transformation.

### *4.1. Simulation of PPG signals with known PRV information*

Simulation of PPG signals opens the door for the development and assessment of novel algorithms and techniques that aid in a more efficient and reliable analysis of the PPG [25,26]. This is due to the capability of simulating a large number of signals with varying features, such as sampling rate, mean heart rate or the quality of the signal. Moreover, it allows for the analysis of signals in a controlled environment, in which no physiological or environmental factors can affect the information obtained from PPG signals.

Different mathematical models have been proposed in the literature for the simulation of PPG signals. As in the model used for this study, Tang et al. [25,26] and Martín-Martínez et al. [39] proposed simulating PPG signals based on the summation of two independent Gaussian functions, whereas other models have used more Gaussian functions for the simulation and parameter estimation of PPG signals [40–42]. The selection of the 2 Gaussian models for this study was based on the simplicity for modelling a single pulse with a given duration. Moreover, the quality of the simulated signal in the proposed model can be varied by changing the ratio

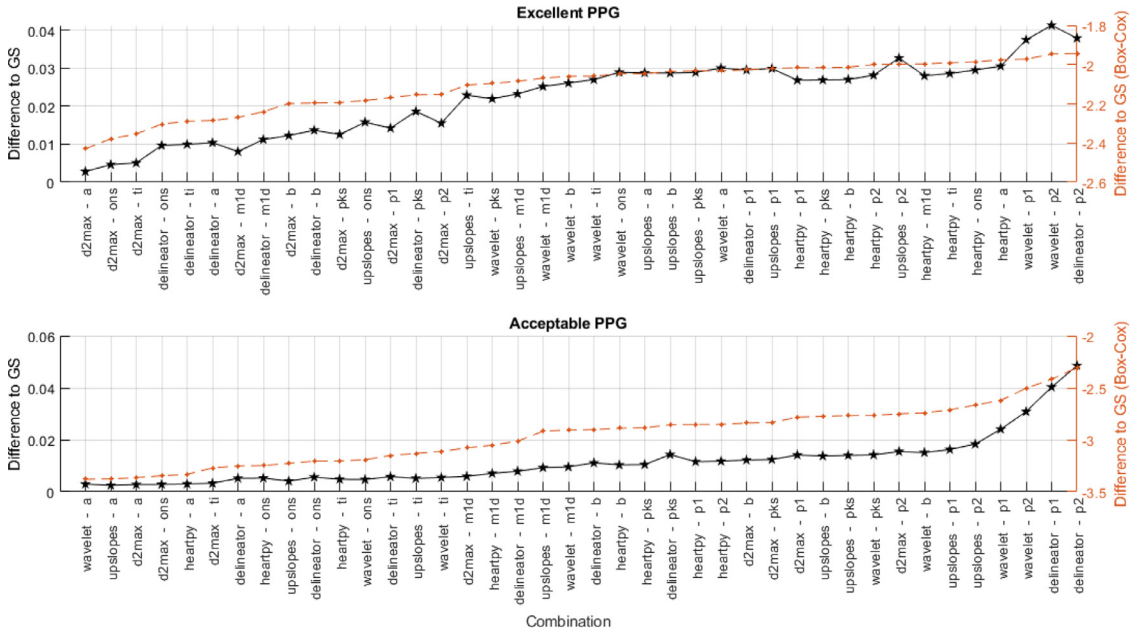


**Fig. 12.** Mean value of the absolute differences between SD1/SD2 measured from gold standard and extracted pulse rate variability (PRV), measured from excellent (top) and acceptable (bottom) quality photoplethysmographic signals. Left axis (black, continuous line): Difference to gold standard before Box-Cox transformations. Right axis (orange, dashed line): Difference to gold standard after Box-Cox transformation.

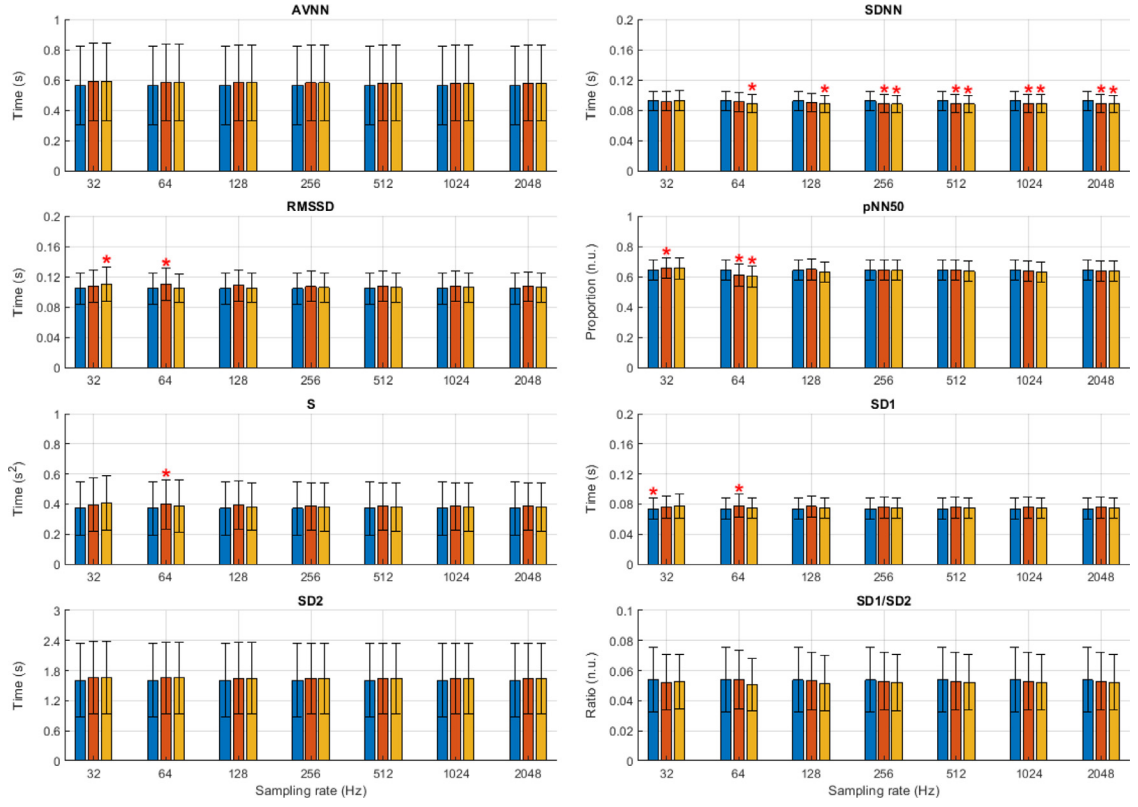


**Fig. 13.** Mean and standard deviation values of time-domain and Poincaré plot indices extracted from pulse rate variability (PRV), both from excellent and acceptable quality simulated photoplethysmographic (PPG) signals, with varying sampling rates. Blue bars: values obtained from gold-standard PRV; orange bars: values obtained from PRV extracted from excellent quality PPG signals; yellow bars: values obtained from PRV extracted from acceptable quality PPG signals. Red stars indicate statistically significant difference to gold standard.

**Table 2**
Results of the post-hoc comparisons between the combination of algorithms and fiducial points with the five lowest differences to the gold standard for each time-domain index extracted from excellent and acceptable quality photoplethysmographic (PPG) signals. (-): Non-significant difference. (+): Significant differences.

| Index | Excellent PPG | | | | | | Acceptable PPG | | | | | |
|---|---|---|---|---|---|---|---|---|---|---|---|---|
| SDNN | | d2max - a | d2max - ons | delineator - ons | d2max - ti | delineator - a | | d2max - a | d2max - ons | delineator - ons | d2max - ti | delineator - a |
| | d2max - a | - | - | - | - | + | d2max - a | - | - | - | - | - |
| | d2max - ons | - | - | - | - | - | d2max - ons | - | - | - | - | - |
| | delineator - ons | - | - | - | - | - | delineator - ons | - | - | - | - | - |
| | d2max - ti | - | - | - | - | - | d2max - ti | - | - | - | - | - |
| | delineator - a | + | - | - | - | - | delineator - a | - | - | - | - | - |
| RMSSD | | d2max - a | d2max - ons | d2max - ti | d2max - m1d | delineator - ons | | d2max - a | d2max - ons | d2max - ti | d2max - m1d | delineator - ons |
| | d2max - a | - | - | - | + | + | d2max - a | - | - | - | + | + |
| | d2max - ons | - | - | - | + | + | d2max - ons | - | - | - | + | + |
| | d2max - ti | - | - | - | + | + | d2max - ti | - | - | - | + | - |
| | d2max - m1d | + | + | + | - | - | d2max - m1d | + | + | + | - | - |
| | delineator - ons | + | + | + | - | - | delineator - ons | + | + | - | - | - |
| pNN50 | | wavelet - ons | d2max - a | heartpy - ti | wavelet - ti | heartpy - ons | | wavelet - ons | d2max - a | heartpy - ti | wavelet - ti | heartpy - ons |
| | wavelet - ons | - | - | - | - | - | wavelet - ons | - | + | - | + | + |
| | d2max - a | - | - | - | - | - | d2max - a | + | - | + | + | - |
| | heartpy - ti | - | - | - | - | - | heartpy - ti | - | + | - | + | + |
| | wavelet - ti | - | - | - | - | - | wavelet - ti | + | + | + | - | + |
| | heartpy - ons | - | - | - | - | - | heartpy - ons | + | - | + | + | - |



**Table 3**
Results of the post-hoc comparisons between the combination of algorithms and fiducial points with the five lowest differences to the gold standard for each Poincaré-plot index extracted from excellent and acceptable quality photoplethysmographic (PPG) signals. (-): Non-significant difference. (+): Significant differences.

| Index | Excellent PPG | | | | | | Acceptable PPG | | | | | |
|---|---|---|---|---|---|---|---|---|---|---|---|---|
| S | | d2max - ons | d2max - ti | d2max - a | d2max - m1d | d2max - b | | d2max - ons | d2max - ti | d2max - a | d2max - m1d | d2max - b |
| | d2max - ons | - | - | - | + | + | d2max - ons | - | - | - | + | + |
| | d2max - ti | - | - | - | + | + | d2max - ti | - | - | - | - | + |
| | d2max - a | - | - | - | - | + | d2max - a | - | - | - | + | + |
| | d2max - m1d | + | + | - | - | - | d2max - m1d | + | - | + | - | + |
| | d2max - b | + | + | + | - | - | d2max - b | + | + | + | + | - |
| SD1 | | d2max - a | d2max - ons | d2max - ti | d2max - m1d | delineator - ons | | d2max - a | d2max - ons | d2max - ti | d2max - m1d | delineator - ons |
| | d2max - a | - | - | - | + | + | d2max - a | - | - | - | + | + |
| | d2max - ons | - | - | - | + | + | d2max - ons | - | - | - | + | + |
| | d2max - ti | - | - | - | + | + | d2max - ti | - | - | - | + | - |
| | d2max - m1d | + | + | + | - | - | d2max - m1d | + | + | + | - | - |
| | delineator - ons | + | + | + | - | - | delineator - ons | + | + | - | - | - |
| SD1/SD2 | | d2max - a | d2max - ons | d2max - ti | delineator - ons | delineator - ti | | d2max - a | d2max - ons | d2max - ti | delineator - ons | delineator - ti |
| | d2max - a | - | - | - | + | + | d2max - a | - | - | - | + | + |
| | d2max - ons | - | - | - | - | - | d2max - ons | - | - | - | - | + |
| | d2max - ti | - | - | - | - | - | d2max - ti | - | - | - | - | - |
| | delineator - ons | + | - | - | - | - | delineator - ons | + | - | - | - | - |
| | delineator - ti | + | - | - | - | - | delineator - ti | + | + | - | - | - |

of amplitudes of the Gaussian functions, which allow for the simulation of PPG signals with varying morphology, which could more reliably simulate signals acquired from different body sites, such as the earlobe or the neck [43], or with varying vascular conditions, such as ageing [44]. Being able to simulate PPG signals with varying morphology could also allow for other studies, such as the development of signal quality indices for PPG signals measured from different body sites [45].

Since the main aim of this study was to evaluate the effects of some technical aspects on PRV information extracted from PPG, the duration of the pulses for the simulated PPG signals were determined using a sinusoidal wave with randomly selected features, i.e., random amplitude, frequency content and offset. Each of these features were related to specific PRV indices: The amplitude relates to the standard deviation of the inter-beat intervals, SDNN; the frequency content was determined to belong in the frequency bands of interest for short-term PRV analysis (i.e. low- and high-frequency bands, LF and HF); and the offset relates to the average duration of the inter-beat intervals, AVNN. Therefore, these parameters were generated in specific ranges that could be observed in human beings.

By comparing the results obtained after processing the simulated signals to known features from the simulated PRV information, it was possible to evaluate the effects of some of these technical aspects on PRV, specifically the algorithms and fiducial points used to detect cardiac cycles and the sampling rate used to acquire PPG signals, in the absence of other confounding factors, such as movement or respiration. Although these aspects may alter the technical aspects of PRV analysis, they also have a physiological effect that may confound results of similar studies when PRV is obtained from real PPG signals and compared to ECG-derived HRV. Hence, although similar studies can be found in the literature, the validation of these factors in these studies is based on the comparison between PRV- and HRV-related indices, with HRV extracted from ECG signals considered as the gold standard. As has been mentioned, although PRV and HRV have a similar origin and HR and PR can be used as surrogates [1], HRV and PRV are not always the same, and by comparing indices extracted from these two techniques, a bias could be introduced in the results. Hence, using simulated PPG signals with known PRV information allows for an unbiased assessment of technical aspects related to the acquisition and processing of PPG signals for the analysis of PRV information.

### *4.2. Experiment 1: Selection of the best combination of cardiac cycles detection algorithm and fiducial point*

The first experiment performed in this study aimed to determine the effects of changing the inter-beat intervals detection algorithm and the fiducial points used for the extraction of PRV from PPG signals.

In general, it was observed that D2Max outperformed the other evaluated algorithms, especially when onset-related fiducial points were used, i.e., the A point from the second derivative of the PPG, the valley (ONS), and the intersection point of the tangent lines (TI) of the PPG. On the other hand, the combination of HeartPy and A points, for excellent PPG quality, and Delineator and P2 points, for acceptable PPG quality, were the algorithms and fiducial points that showed the worst performance for extracting PRV indices. In line with previous studies that have shown that PPG can be used to reliably estimate HR [6], AVNN and SD2, which has been shown to reflect the same processes from the PRV [33], did not show a significant effect when the fiducial points were modified. Therefore, these indices could be extracted reliably from PRV traces derived using any of these fiducial points.

Although the combination of algorithms and fiducial points selected could affect the extracted indices, it is important to notice that most of the best performing combinations did not show statistically significant differences among them, opening a variety of options for the extraction of PRV from PPG signals, which could depend on several factors for the selection of the best combination for a given application, such as the computing power available, the indices of interest and the expected signal quality. Other algorithms and fiducial points have been proposed in the literature, and could give different results. However, it is evident that fiducial points related to the onset of the pulse tend to perform better, as do algorithms that are based on the identification for these points for the segmentation of inter-beat intervals from the PPG signal.

Similar studies can be found in the literature, in which authors compared PRV indices extracted from PPG using different fiducial points for the estimation of inter-beat intervals. Posada-Quintero et al. [18] and Hemon and Phillips [19] found a better performance when PRV was extracted from TI points, while Pinheiro et al. [46] concluded that using the time instants corresponding to 50%, 80% and the maximum peak amplitude of the PPG waveform resulted in less errors for measuring PRV. Although the results obtained by Pinheiro et al. do not correspond to those obtained in this experiment, they also concluded that the selection of the best fiducial point to use depended on the context, which is in line with the differences observed between PRV extracted from excellent and acceptable quality PPG signals. This same conclusion has been achieved by Peralta et al. [47], who found that there are differences in the performance of PRV extracted from several fiducial points when signals are obtained from the finger and the forehead, and they concluded that there is a need to define the fiducial points with best performance under different circumstances. In their results, they found that the middle amplitude point of the PPG signal, M1D and TI points have the best accuracy for PRV analysis. In these studies, however, the comparison was made between HRV and PRV indices, and the number of signals used in each study were limited.

Regarding the analysis of the best performing algorithms for PRV analysis, studies reported in the literature are much more scarce. In 2020, Argüello Prada and Paredes Higinio analysed the differences between a modified version of Upslopes and detecting cardiac cycles by identifying the maximum of the first derivative of the PPG signal, to determine PRV from PPG signals with sudden decreases in the signal amplitude [48]. They found that the modified version of their algorithm, which they called MMPD, had better performance for detecting the sudden amplitude changes in PPG signals, while also gave better results in terms of PRV, although the differences were relatively small except for pNN50. In a similar analysis, Koch et al. evaluated the performance of their algorithm for PRV analysis [49]. They applied their algorithm, which is based on the detection of systolic peaks from the PPG using artificial neural networks, for the extraction of PRV indices from PPG signals included in two publicly available databases, and found that it performed better when compared to two reference algorithms, i.e., an automatic multiscale-based peak detection (AMPD) and a decision tree-based peak detection (DTPD), especially when noisy PPG signals were involved. However, in both cases, the details about how the reference algorithms were applied is not included.

In the case of the algorithms used in the present study, their performance has been evaluated according to their sensitivity (*Sen*), positive predictivity ($P+$) and root-mean-square error (RMSE) for the detection of cardiac cycles. Li et al. found a *Sen* of 99.43%, a $P+$ of 99.45% and an average error rate of 1.14% for Delineator when applied to arterial blood pressure waveforms [31]; Conn and Borkholder reported $Sen = 99.29\%$ and $P+ = 99.23\%$, with a temporal accuracy of $3.8 \pm 2.6$ ms when their algorithm, Wavelet, was applied to PPG signals acquired from 13 subjects while exercising on a bike [30]; van Gent et al. re-

ported RMSE for HeartPy when comparing the developed algorithm against the annotations from a PPG dataset with 20.7 h of recordings, and found that, when compared against other algorithms available in the literature (i.e., the Pan-Tompkins and HRVAS ECGViewer algorithms), HeartPy had lower errors for peak location (0.89 ms), RMSE for peak-to-peak intervals (29.64), RMSE for beats per minute (3.77) and RMSE for SDSD (167.77) [27]; Elgendi et al. reported $Sen = 99.84\%$ and $P+ = 99.89\%$ for D2max, when signals obtained from 40 healthy subjects under challenging conditions, and claim that D2max have comparable performance to other algorithms even if it showed lower accuracy [28]; while Argüello Prada and Serna Maldonado reported $Se = 99.75\%$, $P+ = 98.02\%$ and a Failure Detection Rate (FDR) of 0.02% for Upslopes, concluding that their algorithm performed better than a benchmark algorithm and two previous versions of their own algorithm, when tested using two pediatric PPG recordings [29]. The only case in which an index from PRV was assessed for any of these algorithms was for HeartPy, and all of these algorithms were evaluated under different circumstances and databases. To the best of the knowledge of the authors, there have not been any studies that aimed to find the best combination of algorithms and fiducial points for the extraction of PRV information from PPG signals.

### 4.3. Experiment 2: Effects of lowering sampling rate for the extraction of pulse rate variability

Using lower sampling rates for the extraction of PRV from PPG signals is highly desirable, especially for the continuous measurement of PRV indices in real-time scenarios using wearable devices or video-based PPG signals. From the second experiment performed in this study, it can be observed that, in most cases, the higher the sampling rate, the better performance for the extraction of PRV information. However, for most indices, the sampling frequency can be lowered to around 128 Hz, compared to the sampling rate suggested for HRV analysis (above 1 kHz [24]). Moreover, for applications in which obtaining the instant heart rate is the aim, having sampling rates as low as 32 Hz does not significantly affect the results. Hence, the selection of sampling rate depends on the intended application, but can be around 8 times lower than that suggested for HRV analysis from ECG, which could save resources especially in real-time scenarios.

The results obtained for SDNN show an unexpected behaviour, in which increasing sampling rate affects the results obtained, showing a significant difference between the gold standard and the extracted PRV. More studies should aim to understand this behaviour, but it could be related to the way PRV information is being simulated in the model applied in this study.

Previous studies have aimed to understand how using lower sampling rates may affect PRV-related indices. Choi and Shin [21] found that a sampling rate as low as 25 Hz was appropriate for the extraction of several PRV indices, while Ahn and Kim [50] suggested that the sampling rate of PPG signals should not be lowered than 500 Hz for PRV analysis, after they compared HRV and PRV tachograms using cross-correlation. Also, Béres and Hejjel [51] found that, as has been observed in this study, the sampling rate needed depends on the indices of interest, with a sampling rate as low as 5 Hz for the estimation of AVNN, and a sampling interval of at least 20 ms for the estimation of SDNN and RMSSD without interpolation of the PPG signal. In line with this study, the results obtained suggest that the sampling rate should be higher than 64 Hz for obtaining reliable results. As before, these previous studies were performed comparing HRV and PRV indices from smaller databases, unlike the results obtained in this experiment, in which PRV was compared to a known value and from a larger database, where the sample size was statistically determined. Therefore, there might be differences among the results and the conclusions that can relate to these two factors.

It is important to mention that reducing the sampling rate below the suggested values does not imply that PRV analysis cannot be performed. If PPG is acquired using low sampling rates, interpolation can be used to increase the performance for PRV measurement, as suggested by Béres, Holczer and Hejjel [51,52], while other alternatives have been suggested, such as the parabola approximation method [23,51], curve fitting [53], or other interval compensation methods [54].

### 4.4. Limitations of the study

There are some limitations in this study. First of all, regardless of the benefits of using simulated signals, there are also possible limitations that can relate to this fact. Specifically, using simulated PPG signals may not represent the entire variation of the PPG morphology. However, the model used in this study is based on parameters obtained from PPG signals obtained from real patients, as explained in [25,26]. The simulation of PRV information may also affect the results obtained. However, PRV was simulated using physiologically feasible values, which may introduce larger variability of the PRV but also simulate PRV information that could be obtained from most of the healthy population. Also, it is important to notice that the simulated PPG signals were almost ideal, without any noise or additional physiological aspects, such as respiration or arterial stiffness, that could modify the quality of the PPG. These results, therefore, should later be validated with real data or with simulated signals which take into account these kind of artefacts that are usually expected in PPG signals. In addition, the PRV analysis performed in these studies was limited to time domain and Poincaré plot indices. While frequency-domain indices are probably the most common indices used in the literature, it was decided not to use them in these experiments due to additional parameters that are needed for performing spectral analysis of PRV information, which should also be validated, such as the algorithm used for spectral analysis; the interpolation used before obtaining the spectra, if needed; and the number of points used for the assessment of frequency spectra. Further studies should aim to evaluate and assess the effects of modifying these parameters for frequency-domain analysis of PRV. Finally, the analysis performed with the different algorithms did not include any measurement of sensitivity and specificity for detecting cardiac cycles. This was mainly due to the fact that there were no annotations regarding cardiac cycle locations for this analysis, which could be used as reference. Moreover, the aim of the analysis was to obtain the best combination of algorithms and fiducial points to use specifically for PRV analysis. The sensitivity and specificity analysis for these algorithms should be performed in future studies.

## 5. Conclusion

Pulse rate variability has been largely used for the assessment of HRV information, although their relationship is not yet clear. Moreover, the ever-increasing application of PPG sensors and analysis from wearable and low-cost devices in real life scenarios, make PRV a valuable variable that could be used for assessing health and life quality in a continuous manner. However, there has not been a standardisation of methodologies for the acquisition and processing of PPG signals for the analysis of PRV. In this study, simulated PPG signals with known PRV values were used for evaluating the performance of inter-beat intervals detection algorithms and fiducial points, as well as the effects of lowering PPG sampling rate, for the assessment of PRV indices. It was found that algorithms and fiducial points based on the valley point from the PPG signal performed better for the extraction of most indices, while

lowering sampling rates to around 128 Hz allowed for a good estimation of all indices except SDNN. Further studies should aim to evaluate this results in real PPG signals and with PPG signals with different artefacts. Moreover, frequency-domain indices should be included after assessing which is the best way to extract frequency spectra from PRV information.

## Declaration of Competing Interest

The authors declare that they have no known competing financial interests or personal relationships that could have appeared to influence the work reported in this paper.

## References


[1] E. Mejía-Mejía, J. May, R. Torres, P. Kyriacou, Pulse rate variability in cardiovascular health: a review on its applications and relationship with heart rate variability, Physiol. Meas. 41 (2020) 07TR01, doi:10.1088/1361-6579/ab998c.

[2] H. Huikuri, T. Mäkikallio, K. Airaksinen, R. Mitrani, A. Castellanos, R. Myerburg, Measurement of Heart Rate Variability: A Clinical Tool or a Research Toy? J. Am. Coll. Cardiol. 34 (7) (1999) 1878–1883, doi:10.1016/s0735-1097(99)00468-4.

[3] D. Quintana, Statistical considerations for reporting and planning heart rate variability case-control studies, Psychophysiology 54 (3) (2017) 344–349, doi:10.1111/psyp.12798.

[4] M. Malik, H. Huikuri, F. Lombardi, G. Schmidt, The purpose of heart rate variability measurements, Clin. Aut. Res. 27 (2017) 139–140, doi:10.1007/s10286-017-0416-8.

[5] J. Allen, Photoplethysmography and its application in clinical physiological measurement, Physiol. Meas. 28 (2007) R1–R39, doi:10.1088/0967-3334/28/3/R01.

[6] A. Schäfer, J. Vagedes, How accurate is pulse rate variability as an estimate of heart rate variability? A review on studies comparing photoplethysmographic technology with an electrocardiogram, Int. J. Cardiol. 166 (2013) 15–29, doi:10.1016/j.ijcard.2012.03.119.

[7] N.D. Giardino, P.M. Lehrer, R. Edelberg, Comparison of finger plethysmograph to ECG in the measurement of heart rate variability, Psychophysiology 39 (2002) 246–253, doi:10.1017/S0048577202990049.

[8] K. Charlot, J. Cornolo, J.V. Brugniaux, J.P. Richalet, A. Pichon, Interchangeability between heart rate and photoplethysmography variabilities during sympathetic stimulations, Physiol. Meas. 30 (2009) 1357–1369, doi:10.1088/0967-3334/30/12/005.

[9] A.H. Khandoker, C.K. Karmakar, M. Palaniswami, Comparison of pulse rate variability with heart rate variability during obstructive sleep apnea, Med. Eng. Phys. 33 (2011) 204–209, doi:10.1016/j.medengphy.2010.09.020.

[10] E. Mejía-Mejía, J.M. May, M. Elgendi, P.A. Kyriacou, Differential effects of the blood pressure state on pulse rate variability and heart rate variability in critically ill patients, npj Digit. Med. 4 (2021) 82, doi:10.1038/s41746-021-00447-y.

[11] X. Chen, Y.-Y. Huang, F. Yun, T.-J. Chen, J. Li, Effect of changes in sympathovagal balance on the accuracy of heart rate variability obtained from photoplethysmography, Exp. Ther. Med. 10 (2015) 2311–2318, doi:10.3892/etm.2015.2784.

[12] E. Gil, M. Orini, R. Bailón, J.M. Vergara, L. Mainardi, P. Laguna, Photoplethysmography pulse rate variability as a surrogate measurement of heart rate variability during non-stationary conditions, Physiol. Meas. 31 (9) (2010) 1271–1290, doi:10.1088/0967-3334/31/9/015.

[13] I. Trajkovic, F. Scholkmann, M. Wolf, Estimating and validating the interbeat intervals of the heart using near-infrared spectroscopy on the human forehead, J. Biomed. Opt. 16 (2011) 087002, doi:10.1117/1.3606560.

[14] I. Constant, D. Laude, I. Murat, J.-L. Elghozi, Pulse rate variability is not a surrogate for heart rate variability, Clin. Sci. 97 (1999) 391–397.

[15] P.R. Pellegrino, A.M. Schiller, I.H. Zucker, Validation of pulse rate variability as a surrogate for heart rate variability in chronically instrumented rabbits, Am. J. Physiol. Heart Circ. Physiol. 307 (2014) H97–H109, doi:10.1152/ajpheart.00898.2013.

[16] E. Yuda, K. Yamamoto, Y. Yoshida, J. Hayano, Differences in pulse rate variability with measurement site, J. Physiol. Anthropol. 39 (2020) 4, doi:10.1186/s40101-020-0214-1.

[17] E. Mejía-Mejía, K. Budidha, T. Abay, J. May, P. Kyriacou, Heart Rate Variability (HRV) and Pulse Rate Variability (PRV) for the Assessment of Autonomic Responses, Front. Physiol. 11 (2020) 779, doi:10.3389/fphys.2020.00779.

[18] H.F. Posada-Quintero, D. Delisle-Rodríguez, M.B. Cuadra-Sanz, R.R.F. de la Vara-Prieto, Evaluation of pulse rate variability obtained by the pulse onsets of the photoplethysmographic signal, Physiol. Meas. 34 (2) (2013) 179–187, doi:10.1088/0967-3334/34/2/179.

[19] M.C. Hemon, J.P. Phillips, Comparison of foot finding methods for deriving instantaneous pulse rates from photoplethysmographic signals, J. Clin. Monit. Comput. 30 (2) (2016) 157–168, doi:10.1007/s10877-015-9695-6.

[20] A. Alqaraawi, A. Alwosheel, A. Alasaad, Heart rate variability estimation in photoplethysmography signals using Bayesian learning approach, Healthcare Technol. Lett. 3 (2) (2016) 136–142, doi:10.1049/htl.2016.0006.

[21] A. Choi, H. Shin, Photoplethysmography sampling frequency: pilot assessment ofhow low can we go to analyze pulse rate variability with reliability? Physiol. Meas. 38 (3) (2017) 586–600, doi:10.1088/1361-6579/aa5efa.

[22] L. Hejjel, Comment on 'Photoplethysmography sampling frequency: pilot assessment ofhow low can we go to analyze pulse rate variability with reliability?', Physiol. Meas. 38 (12) (2017) 2249–2251, doi:10.1088/1361-6579/aa9303.

[23] H.J. Baek, J. Shin, G. Jin, J. Cho, Reliability of the parabola approximation method in heart rate variability analysis using low-sampling-rate photoplethysmography, J. Med. Syst. 41 (12) (2017) 189, doi:10.1007/s10916-017-0842-0.

[24] Task Force of the European Society of Cardiology and The North American Society of Pacing and Electrophysiology, Heart rate variability: Standards of measurement, physiological interpretation, and clinical use, Circulation 93 (1996) 1043–1065, doi:10.1161/01.CIR.93.5.1043.

[25] Q. Tang, Z. Chen, R. Ward, M. Elgendi, Synthetic photoplethysmogram generation using two Gaussian functions, Sci. Rep. 10 (2020) 13883, doi:10.1038/s41598-020-69076-x.

[26] Q. Tang, Z. Chen, J. Allen, A. Alian, C. Menon, R. Ward, M. Elgendi, PPGSynth: An Innovative Toolbox for Synthesizing Regular and Irregular Photoplethysmography Waveforms, Front Med (Lausanne) 7 (2020) 597774, doi:10.3389/fmed.2020.597774.

[27] P. van Gent, H. Farah, N. van Nesb, B. Arem, HeartPy: A novel heart rate algorithm for the analysis of noisy signals, Transp. Res. F: Traffic Psychol. Behav. 66 (2019) 368–378, doi:10.1016/j.trf.2019.09.015.

[28] M. Elgendi, I. Norton, M. Brearley, D. Abbott, D. Schuurmans, Systolic peak detection in acceleration photoplethysmograms measured from emergency responders in tropical conditions, PLoS One 8 (10) (2013) e76585, doi:10.1371/journal.pone.0076585.

[29] E.A. Prada, R.S. Maldonado, A novel and low-complexity peak detection algorithm for heart rate estimation from low-amplitude photoplethysmographic (PPG) signals, J. Med. Eng. Technol. 42 (8) (2018) 569–577, doi:10.1080/03091902.2019.1572237.

[30] N. Conn, D. Borkholder, Wavelet based photoplethysmogram foot delineation for heart rate variability applications, in: 2013 IEEE Signal Processing in Medicine and Biology Symposium (SPMB), 2013, pp. 1–5, doi:10.1109/SPMB.2013.6736782.

[31] B. Li, M. Dong, M. Vai, On an automatic delineator for arterial blood pressure waveforms, Biomed. Signal Process. Control 5 (2010) 76–81, doi:10.1016/j.bspc.2009.06.002.

[32] E. Mejía-Mejía, J. Allen, K. Budidha, C. El-Hajja, P. Kyriacou, P. Charlton, Photoplethysmography signal processing and synthesis, in: P. Kyriacou, J. Allen (Eds.), Photoplethysmography: Technology, Signal Analysis, and Applications, Elsevier, London, UK, 2021, pp. 69–145.

[33] A. Khandoker, C. Karmakar, M. Brennan, A. Voss, M. Palaniswami, Poincaré Plot Methods for Heart Rate Variability Analysis, Springer, New York, NY, 2013, doi:10.1007/978-1-4614-7375-6.

[34] S. Alvarado Orellana, Aportes metodológicos en la estimación de tamaños de muestra en estudios poblacionales de prevalencia, Universitat Autònoma de Barcelona, Cerdanyola del Vallès, Barcelona, 2014 Ph.D. thesis.

[35] K.-M. Colimon, Fundamentos de Epidemiología, 3, ECOE Ediciones, Bogotá, Colombia, 2018.

[36] J. Khalilzadeh, A. Tasci, Large sample size, significance level, and the effect size: Solutions to perils of using big data for academic research, Tour. Manag. 62 (2017) 89–96, doi:10.1016/j.tourman.2017.03.026.

[37] R. Kaplan, D. Chambers, R. Glasgow, Big data and large sample size: a cautionary note on the potential for bias, Clin. Transl. Sci. 7 (4) (2014) 342–346, doi:10.1111/cts.12178.

[38] G. Box, D. Cox, An analysis of transformations, J. R. Stat. Soc. Series B Stat. Methodol. (1964) 211–252.

[39] D. Martín-Martínez, P. Casaseca-de-la Higuera, M. Martín-Fernández, C. Alberola-López, "stochastic modeling of the ppg signal: A synthesis-by-analysis approach with applications", IEEE Trans. Biomed. Eng. 60 (9) (2013) 2432–2441, doi:10.1109/TBME.2013.2257770.

[40] U. Rubins, Finger and ear photoplethysmogram waveform analysis by fitting with gaussians, Med. Biol. Eng. Comput 46 (2008) 1271–1276, doi:10.1007/s11517-008-0406-z.

[41] L. Wang, L. Xu, S. Feng, M.Q.-H. Meng, K. Wang, Multi-gaussian fitting for pulse waveform using weighted least squares and multi-criteria decision making method, Comput. Biol. Med. 43 (11) (2013) 1661–1672, doi:10.1016/j.compbiomed.2013.08.004.

[42] A. Sološenko, A. Petrėnasa, V. Marozasa, L. Sörnmo, Modeling of the photoplethysmogram during atrial fibrillation, Comput. Biol. Med. 81 (2017) 130–138, doi:10.1016/j.compbiomed.2016.12.016.

[43] P.H. Charlton, J. Mariscal Harana, S. Vennin, Y. Li, P. Chowienczyk, J. Alastruey, Modeling arterial pulse waves in healthy aging: a database for in silico evaluation of hemodynamics and pulse wave indexes, Am. J. Physiol. Heart Circ. Physiol. 317 (5) (2019) H1062–H1085, doi:10.1152/ajpheart.00218.201.

[44] J. Allen, A. Murray, Age-related changes in the characteristics of the photoplethysmographic pulse shape at various body sites, Physiol. Meas. 21 (2) (2003) 297–307, doi:10.1088/0967-3334/24/2/306.

[45] M. Nardelli, N. Vanello, G. Galperti, A. Greco, E. Scilingo, Assessing the quality of heart rate variability estimated from wrist and finger ppg: A novel approach based on cross-mapping method, Sensors (Basel) 20 (2020) 3156, doi:10.3390/s20113156.

[46] N. Pinheiro, R. Couceiro, J. Henriques, J. Muehlsteff, I. Quintal, L. Gonçalves, P. Carvalho, Can ppg be used for hrv analysis? in: Annu. Int. Conf. IEEE Eng. Med. Biol. Soc., 2016, pp. 2945–2949, doi:10.1109/EMBC.2016.7591347.

[47] E. Peralta, J. Lazaro, R. Bailon, V. Marozas, E. Gil, Optimal fiducial points for pulse rate variability analysis from forehead and finger photoplethys-

mographic signals, Physiol. Meas. 40 (2019) 025007, doi:10.1088/1361-6579/ab009b.
[48] E. Argüello Prada, A. Paredes Higinio, A low-complexity ppg pulse detection method for accurate estimation of the pulse rate variability (prv) during sudden decreases in the signal amplitude, Physiol Meas 41 (2020) 035001, doi:10.1088/1361-6579/ab7878.
[49] R. Koch, N. Pfeiffer, N. Lang, B. Eskofier, O. Amft, M. Struck, T. Wittenberg, Evaluation of hrv estimation algorithms from ppg data using neural networks, Curr Dir Biomed Eng 6 (2020) 505–509, doi:10.1515/cdbme-2020-3130.
[50] J.M. Ahn, J.K. Kim, Effect of the ppg sampling frequency of an iir filter on heart rate variability parameters, Int. J. Sci. Technol. Res. 9 (3) (2020) 1933–1937.
[51] S. Béres, L. Hejjel, The minimal sampling frequency of the photoplethysmogram for accurate pulse rate variability parameters in healthy volunteers, Biomed. Signal Process. Control 68 (2021) 102589, doi:10.1016/j.bspc.2021.102589.
[52] S. Béres, L. Holczer, L. Hejjel, On the minimal adequate sampling frequency of the photoplethysmogram for pulse rate monitoring and heart rate variability analysis in mobile and wearable technology, Meas Sci Rev 19 (2019) 232–240, doi:10.2478/msr-2019-0030.
[53] F. Panganiban, F. de Leon, Reducing pulse rate variability computational error from a 30 hz photoplethysmography recording, in: 2019 International Symposium on Multimedia and Communication Technology (ISMAC), 2019, pp. 1–6, doi:10.1109/ISMAC.2019.8836186.
[54] K. Watanabe, S. Izumi, Y. Yano, H. Kawaguchi, M. Yoshimoto, Heartbeat interval error compensation method for low sampling rates photoplethysmography sensors, IEICE Trans. Commun. E103-B (2020) 645–652, doi:10.1587/transcom.2019HMP0002.